STM JOURNALS

Journal of
Electro-Mechanics and
Material Behaviour

Volume 2, Issue 1, 2024
January–June
DOI Journal: 10.37591/IJEMB

https://journals.stmjournals.com/ijemb

Research IJEMB

Management of Lead–Acid Battery System in Electric Vehicles

Arun Kumar[1], Sushil Kumar Agrawal[2], Rachit Srivastava[3], Jay Bahadur Singh[3], Tej Prakash Verma[3], Palak Gaur[4,*]

Abstract

To determine the lead-acid battery's state of charge in electric vehicles, a novel coulometric method is presented in this article. There are two major problems with the main state of charge algorithms that are currently in use: one defines the state of charge incorrectly for applications involving electric vehicles, and the other uses the accumulator's static performance sub-optimally to estimate its state under dynamic stresses. To address these two shortcomings, we suggest a novel coulometric algorithm that is connected to the electric vehicle's performance. The virtually discharged ampere-hours are determined by using statistical equivalency coefficients on the actual current profile. A considerable improvement with less than 5% errors in all cases examined is shown by the evaluation of this new algorithm on actual discharges.

Keywords: Electric vehicles, lead-acid battery, lead corrosion, manufacturers, analytical models

INTRODUCTION

The most popular electrochemical solution for storing electrical energy is a lead-acid battery. The complex processes taking place inside the batteries are still not fully understood, which is why a lot of study is currently being done in this area even if their fundamental physical concept is not new. Manufacturers and consumers encounter challenges as a result, as they may not always be aware of issues that could arise under particular circumstances. These batteries have been in use for a very long period without having any major problems since they we are not exposed to any real substantial limits. Battery performance is widely understood under static conditions (constant temperature and current), but because of the significant amplitude fluctuations in the currents, it varies substantially in applications involving electric cars. In this instance, we wanted to install a new battery gauge for a Volta electric vehicle (Table 1) that has six installed Oldham 6RGT180 batteries. This investigation was carried out by Oldham France and the Ecole Centrale de Lille (L2EP) with financial support from Innovates [1, 2]. Various research approaches can be taken into consideration based on the gauge's kind and complexity.

- Analytical models, finite element models, and analogous electrical circuit models are some modelling techniques [3, 4].

***Author for Correspondence**
Palak Gaur
E-mail: palakgaurtoto@gmail.com

[1]Associate Professor, Department of Electrical Engineering, Bansal Institute of Engineering and Technology, Lucknow, Uttar Pradesh, India
[2]Professor, Department of Electrical Engineering, Bansal Institute of Engineering Technology, Lucknow, Uttar Pradesh, India
[3]Assistant Professor, Department of Electrical Engineering, Bansal Institute of Engineering and Technology, Lucknow, Uttar Pradesh, India
[4]Student, Department of Electrical Engineering, Bansal Institute of Engineering and Technology, Lucknow, Uttar Pradesh, India

Received Date: May 23, 2024
Accepted Date: June 12, 2024
Published Date: June 26, 2024

Citation: Arun Kumar, Sushil Kumar Agrawal, Rachit Srivastava, Jay Bahadur Singh, Tej Prakash Verma, Palak Gaur. Management of Lead–Acid Battery System in Electric Vehicles. International Journal of Electro-Mechanics and Material Behaviour. 2024; 2(1): 18–27p.

- Experimental methods, such as impedance, voltage, coulometric, and electrolyte density measurements [4, 5].

Our work was quickly directed towards coulometric techniques due to the requirement that the principle be as simple as possible because the final solution must be applied to a real system. Although they cannot be used for calculations in real time, other methods have not been entirely disregarded and may be used for routine calibration (impedance measurements).

BATTERY BEHAVIOR

To explain the nonlinear events that occur during battery discharges and to justify the requirement for dynamic testing to calibrate the gauge, a basic examination of the accumulator's physio-chemical characteristics is provided before any algorithms are recommended. An elementary model of the chemical transition is offered here to aid in the comprehension and avoidance of gauge-related problems.

Sphere Model

We present a full load model [5, 6] of the positive electrode, which is primarily made of PbO_2 (positive active mass). The electrolyte H_2SO_4 reacts with PbO_2 during discharge to turn it into $PbSO_4$ [6, 7].

$$PbO_2 + HSO_4^- + 2e^- \leftrightarrow PbSO_4 + 2H_2O \quad (1)$$

An assembly of spheres, which stand in for the PbO_2 molecules, is used to model the active mass of this electrode. This model's view of the positive electrode is depicted in Figure 1. A grain of PbO_2, or microscopic agglomerate of PbO_2 molecules, is represented by each sphere [7–9].

Table 1. Volta characteristics.

Vehicle type	Commercial vehicle
Motorization	Series DC motor with gearbox (4-gear)
Nominal power; maximum power	11 kW; 20 kW
Battery type	16 lead acid batteries Oldham 6 RGT 180 in series
Batteries nominal voltage	96 V
Maximum speed	80 km/h
Empty weight	1300 kg with batteries
Autonomy	120 km at 40 km/h; 90 km at 60 km/h

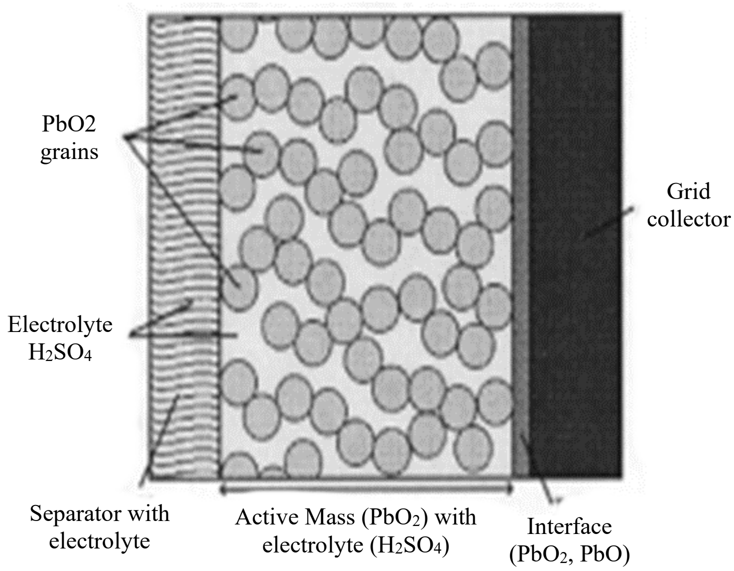

Figure 1. Section view of the positive plate [10].

Discharge Process

PbO molecules are changed into PbSO by the battery discharge, which fills twice the PbO's volume. This change is found in the vicinity of grains. These grains' quantity and location are determined by their reaction time, which is correlated with the discharge current value. The number of transformed grains increases with decreasing current (Figures 2–4) [8, 9].

The battery capacitance value is therefore smaller than it would be with small currents (Figure 5) Fewer ampere hours are provided by the battery the higher the current. This physical impact makes the battery capacitance's agreement to a constant release current clearer (Figure 6).

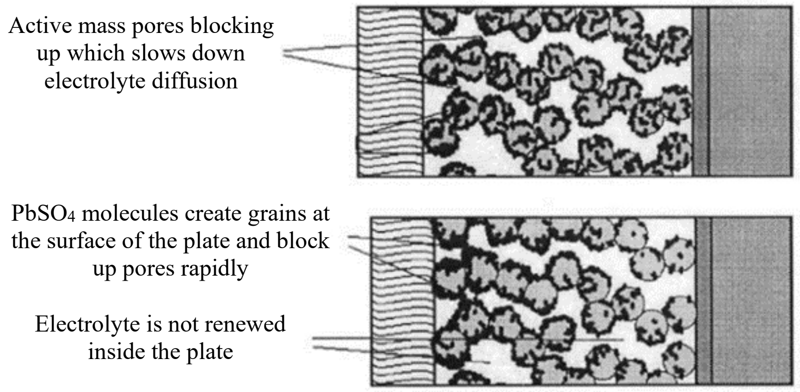

Figure 2. PbO_2 grain composed of PbO_2 molecules [11].

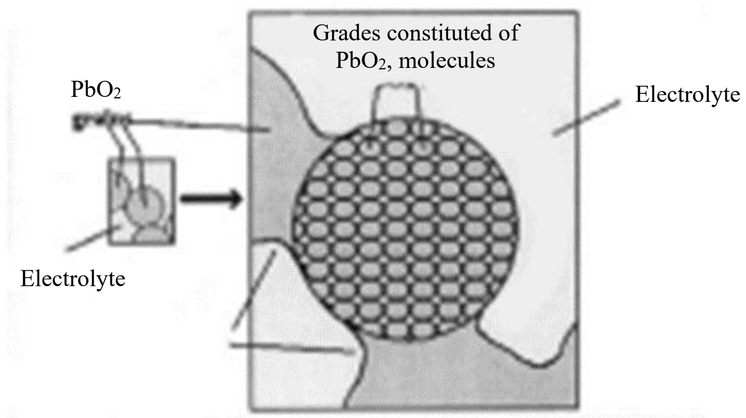

Figure 3. PbO_2 Transformation with a low current battery discharge [12].

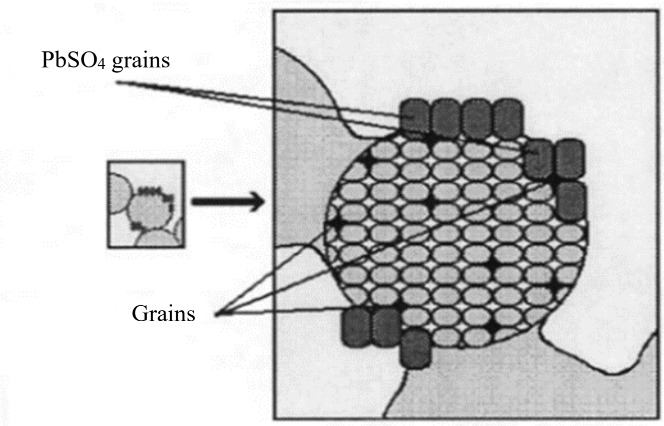

Figure 4. PbO_2 transformation with a high current discharge [13].

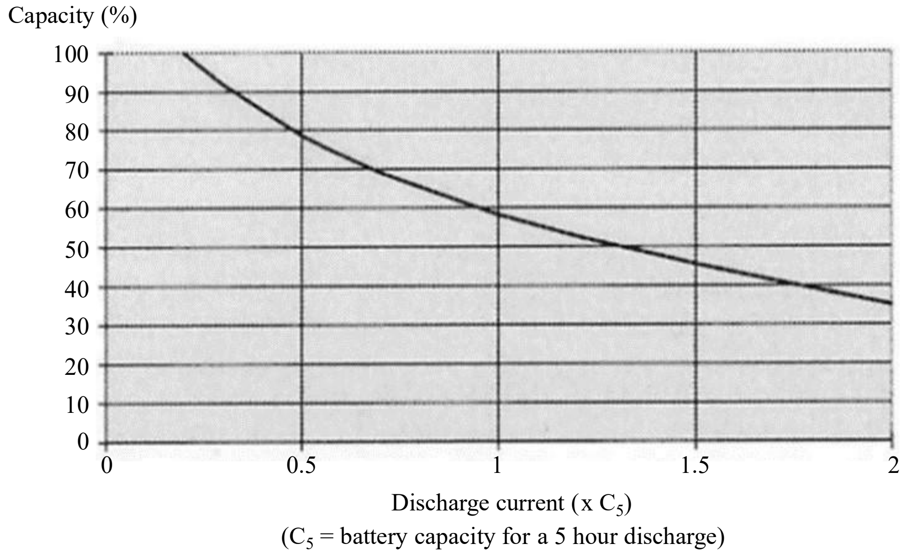

Figure 5. Positive plate at the end of a low current discharge [14].

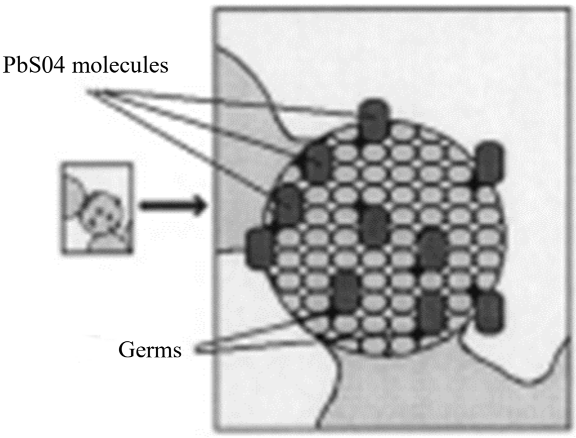

Figure 6. Capacity evolution as a function of the discharge current [15].

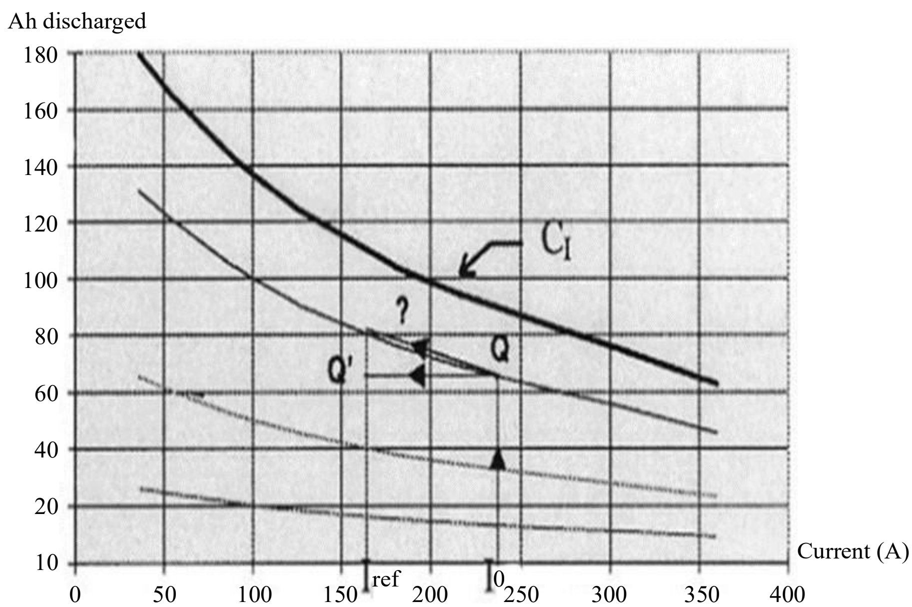

Figure 7. Capacity evolution for a 6RGT180 battery at 25°C [16].

Therefore, if the pores are mainly open, a pause in the release allows the electrolyte to diffuse inside the grains. When the release starts up again, this dispersion permits the dynamic mass to shift, which would not have been altered without stopping, and the battery's capacity is increased. All of these events demonstrate how challenging it is to define an electric car gauge and how many physical factors must be taken into account to get an accurate result (Figure 7).

EVALUATION OF EXISTING COULOMETRIC STATE OF CHARGE ALGORITHMS

We have examined the two primary coulometric algorithms currently in use in gauges to identify their flaws, assess the amplitude of the inaccuracies, and identify fresh trends to enhance them before putting forth a new approach. The first two [17, 18] examine battery capacity at average discharge current, whereas the second set [18, 19] discusses a fixed reference current.

Algorithm Utilizing the Average Discharge Current

The following defines this most popular set of coulometric rules:

- All values are computed at the moment when the preliminary price equals the total fee.
- The total ampere-hours (Ah) that were exchanged during the discharge is indicated as:

$$Q = \int_0^T i(t)\mathrm{dt} \tag{2}$$

Then, at that point, the typical current is effortlessly obtained by:

$$I_a = \frac{Q}{T}$$

By utilizing Figure 7, which gives the full limit as per the current at C, the condition of release (rate) is at last obtained by:

$$S = \frac{Q}{C_{I_a}} \times 100 \tag{3}$$

Method Utilizing a Fixed Reference Current

This type of second calculation measures the extra capacity at a reasonable current (often chosen as the current at the apparent limit for lead-corrosive footing batteries within a 5-hour release period). The computation subtracts the Ampere-hours exchanged, weighted by coefficients that agree with the value of the instant release current, from the maximum of the fully recharged battery at temperature and current. Amperes-hours released at a current cannot be ampere-hours released current (Figure 8) [20, 21].

The definition of the identical released ampere-hours at *t*, the state of charge is prompted by the use of weighting coefficients.

$$Q` = \int_0^T \alpha(i)i(t)dt; \tag{4}$$

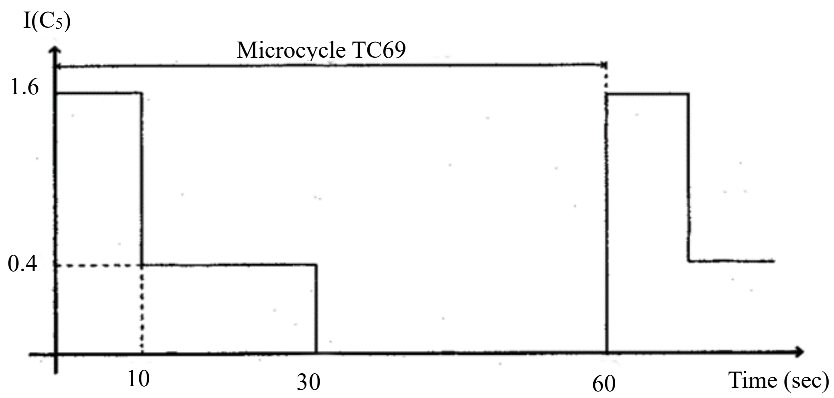

Figure 8. Fixed reference current.

$$S = \frac{Q`}{C_{I_{ref}}} \times 100 \quad (5)$$

The problem lies in figuring out the weighting coefficients' values. The technique by and large utilized depends on the information on the battery execution at steady release current (Figure 7). As a total release at an ongoing prompt a variety of Ah equivalent to contrast with the reference values, a fractional release of Ah prompts:

$$Q` = Q/C_{I0} \cdot \left(C_{I_{ref}} - C_{I0}\right) + Q = Q \cdot C_{I_{ref}}/C_{I0} \quad (6)$$

which gives,

$$\alpha(I_0) = \frac{C_{I_{ref}}}{C_{I0}} \quad (7)$$

This computation is called inside this article.

Evaluation of Both Traditional Algorithms

These labor-intensive computations were tested on a lab test seat using a potent charger-discharger that was coupled to batteries placed in a thermo-field tank at C. At each stage, the major boundaries—temperature, voltage, current, and time—were acquired. A few profiles for releases were selected.

Steady current, JRC-TC69, JRC-ECE-15, and real dynamic discharges (profiles derived from Volta car records). The estimated data on the number of ampere-hours utilized were obtained with an approximate inaccuracy of 0.5% based on one measurement per second. Furthermore, the same attributes hold for future results. Trial and error proceeded at a speed of one cycle (charge-release) each day. The upward conduct of and for this sort of function, which is unrelated to the criteria for electric vehicles, was confirmed by tests conducted with a continuous release current. In this case, the error rate obtained is around 5%, indicating that the system is limited by the boundaries taken into consideration. The old-style TC69 profile is more agent of electric vehicles (Figure 8) [22]. Discharges obtained from the TC69 profile demonstrated positive behavior, but they also showed significant mistakes, which produced a negative gauge:

- with present step lengths tripled (TC3)
- TC69 profile (TC1)

The value of percentage indicated an incomplete battery release because, for the most part, 30% of the battery was still usable (Table 2). In this case, the battery is protected from deep discharge, but it will not satisfy the customer because of its restricted autonomy. Finally, experiments with dynamic current profiles closer to the real-world application of electric vehicles have been conducted, varying depending on the kind of application (urban, rural, mixed). Only these two types of data may be used to define the experimental profiles and rural passengers Volta captured profiles. The Volta's 6RGTI80 batteries, which are in the search canter, have undergone these tests (Table 3). A chosen end-voltage of 1.7 V/cell is used. After this value was obtained, the release was completed at a constant current of 100 Ah until 1.7 V/cell was again attained. This last requirement has been applied to every research facility outcome that is shown here. A is related to the basic value of the continuous signal that the battery provides to ensure that the Volta car operates well in similar traffic situations. Because the findings

Table 2. TC69 results.

Test	TC1	TC2	TC3
IA (C5)	0.4	0.8	0.4
Ah discharged	61.6	53.7	60.4
S with Aa (%)	98.7	104.8	97
S with Aref (%)	131.7	116	131.6

Table 3. Test on dynamic profiles.

Test	Profile	IA	S with A_a	S with Aref
D1	ECE-15, suburban	90.6	97.4	122.60
D2	ECE-15 urban+suburban	65.6	92.5	119.30
D3	ECE-15 urban+suburban	75.8	92.8	119.10
D4	ECE-15, urban	44.2	86.9	119.60
D5	Volta recorded profile	62.3	86.5	117.70

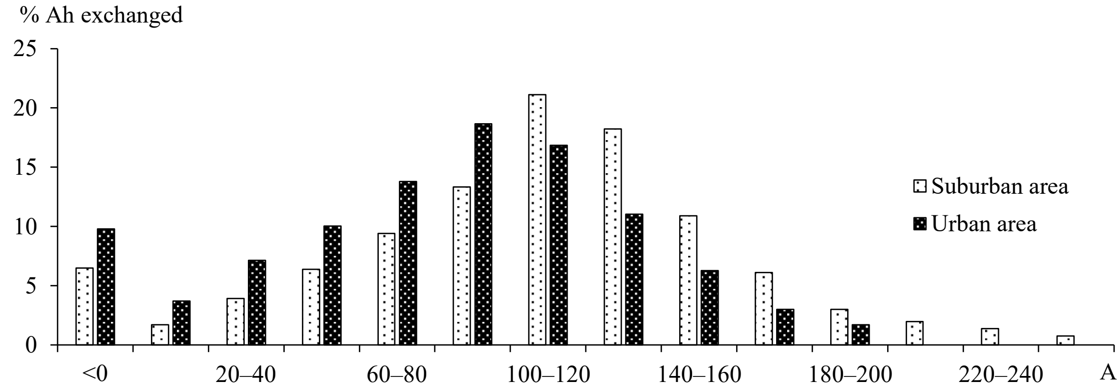

Figure 9. Couple of circumstances.

continue to follow the same pattern, there are around 20% catastrophic errors in almost every situation. Additionally, this causes around 15% of optimistic mistakes in D4 and D5, Trial and error have shown the substandard way of behaving of both algorithms in a couple of circumstances which affirm the need for Figure 9 [23, 24].

Examples of this problem that should not be disregarded are the D4 and DS since they relate to the main application of electric cars, which is the metropolitan cycle. Thus, we suggest doing an additional computation that comes from:

- picking equivalent to ascertain the state of accuse of a reference current which relates to the actual qualities of the vehicle
- applying another strategy
- The term "Ah regenerated by electrolyte diffusion during electric braking and pauses" is now used to describe the new definition of "virtual Ah discharged," as noted at

$$Q(T) = \int_0^T a(i)\, i(t)dt - Q_{reg} \qquad (8)$$

Thus, two unique examinations have been important to determine both new boundaries and which are boundaries considering the battery conduct according to the particular use.

DETERMINATION OF A(I)

This section aims to describe weighting coefficients that are typical of the real application. What distinguishes it is the way the coefficients were computed [25]. We have envisaged testing using dynamic current profiles, instead of using the data from the collector exhibits under static release profiles.

Analysis of Statistical Data

Finding a reasonably adjusted approach is essential to get accurate agent coefficients before attempting trial estimations to determine these attributes. We have accomplished this by doing a factual analysis of the estimates that were documented on board the Volta vehicle to predict the future exploratory profiles that will be used to determine the new coefficients. For example, the distribution by the present level is shown in Figure 10.

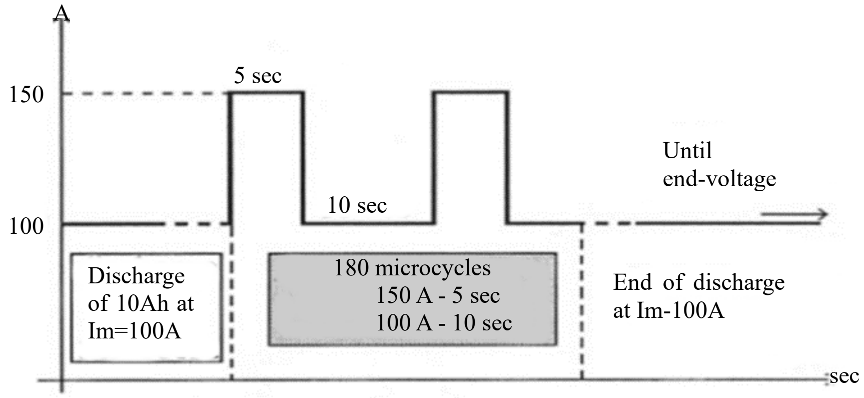

Figure 10. Experimental current profile for the determination of (I = 150 A) [26].

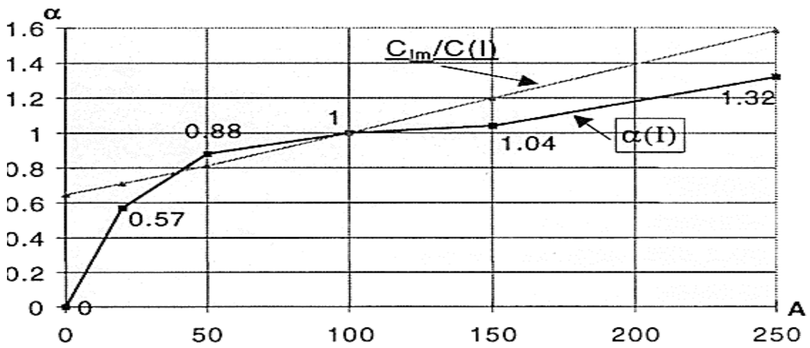

Figure 11. New weighting coefficients [27].

From every one of the outcomes found, the significant snippets of data are:

- The distribution of the current in metropolitan areas results in a Gaussian curve centered on A (Figure 11) [28].
- the typical term of a persistent step of current is around 5 seconds.

Tests on Dynamic Discharge Profiles

To approve the new coefficients, tests under electric vehicle profiles without stops and regenerative slowing down have been carried out by recreating metropolitan use [29, 30]. This strategy prompts a genuine improvement of the traditional algorithms in similar working circumstances. However, assuming that periods of delay and regenerative slowing down are incorporated in the profile, the outcomes (the two models (U2 urban = with pauses, and U-S2 urban + suburban with pauses) yield the same tendency but a larger error [$\alpha(i) = 1$ for $I < 0$]. This last analysis shows that it is important to acquaint another boundary with consideration of better interruption and electrical slowing down.

CONCLUSION

A precise coulometric condition of charge calculation for lead-corrosive batteries in electric vehicles has been created by working on existing strategies with a unique measurable and dynamic methodology. Through well-adapted dynamic tests, statistical coefficients were determined to calculate the ampere-hours discharged at a reference current, which is associated with the minimal performance of the electric vehicle. Regenerative braking and pauses have also been taken into consideration. Based on the parameters that have been taken into consideration, tests of this algorithm on actual discharges have shown that it produces the best results with less than 5% errors. For the future, other notable boundaries must be introduced in the calculation to guarantee its unwavering quality in genuine circumstances for a significant stretch: temperature and maturing impact. Then it will be feasible to fabricate a dependable arrangement of energy control on electric vehicles.

REFERENCES

1. Vasebi A, Bathaee SMT, Partovibakhsh M. Predicting state of charge of lead-acid batteries for hybrid electric vehicles by extended Kalman filter. Energy Convers Manag. 2008;49:75-82. DOI: 10.1016/j.enconman.2007.05.017.
2. Salameh MS, Casacca MA, Lynch WA. A mathematical model for lead-acid batteries. IEEE Trans Energy Convers. 1992; 7 (1): 93–98.
3. Nugues S. Mesure de l'état de charge d'une batterie par coulométrie corrigée par impédancemétrie. Doctoral Thesis. Thèse de doctorat. Grenoble, France: Instituto Politécnico Nacional de Grenoble (INPG); 1996.
4. Smimite H. Etude du comportement et gestion d'une batterie au plomb à recombinaisonéquipant un vehicule électrique. Doctoral Thesis. Thèse de doctorat. Montpellier, France: Université de Montpellier; 1997.
5. Brissaud C. Etude morphologique et structurale des mécanismes de dégradation des batteries plomb-acide à recombinaison de gaz lots des tests de cyclage et de surcharge. Doctoral Thesis. Thèse de doctorat. Lille, France: Université de Lille; 1996.
6. Winsel A, Voss E, Hullmeine U. The aggregate-of-spheres ('Kugelhaufen') model of the $PbO_2/PbSO_4$ electrode. J Power Sources. 1990; 30 (1–4): 209–226.
7. Berndt D. Maintenance-Free Batteries: Lead–Acid, Nickel/Cadmium, Nickel/Hydride — A Handbook of Battery Technology. New York, NY, USA: Wiley-Blackwell; 1993.
8. Bode H. Lead Acid Batteries. New York, NY, USA: Wiley Interscience; 1977.
9. Kiehne HA, Boehm I, Eberts K, et al. Batteries – Fundamentals and Theory, Running Techniques, Outlook. Tübingen, Germany: Expert Verlag; 1989.
10. Karden E, Mauracher P, Lohner A. Battery management system for energy-efficient battery operation: strategy and practical experience. In: 13th International Electric Vehicle Symposium (EVS-13), Osaka, Japan, October 13–16, 1996. p. 91.
11. Song SK, Kim KH. A dynamic state of charge model for electric vehicle batteries. In: 12th International Electric Vehicle Symposium (EVS-12), Anaheim, CA, USA, December 5–7, 1994. pp. 519–527.
12. Guogang Q, Jianming L, Hang J. A new battery state of charge indicator for electric vehicles. In: 13th International Electric Vehicle Symposium (EVS-13), Osaka, Japan, October 13–16, 1996. p. 631.
13. Kitagawa M. Development of battery state of charge indicator for electric vehicles. In: 12th International Electric Vehicle Symposium (EVS-12), Anaheim, CA, USA, December 5–7, 1994. p. 293.
14. Riutort JF. Etude et réalization d'une jauge coulométrique universelle destinée au véhicule électrique. Grenoble, France: Mémoire CNAM Grenoble; 1994.
15. Riutort JF, Rulliere E, Toutain E. An improved coulometric gauge for electric vehicles. Proc Electric Vehicle Technol Conf. 1995; 3: 7–15.
16. Lynch WA, Salameh ZM. Realistic electric vehicle battery evaluation. IEEE Trans. Energy Convers. 1997; 12 (4): 407–412.
17. Affanni A, Bellini A, Franceschini G, Guglielmi P, Tassoni C. Battery choice and management for new-generation electric vehicles. IEEE Trans Indus Electron. 2005; 52 (5): 1343–1349.
18. Zau ATP, Lencwe MJ, Chowdhury SPD, Olwal TO. A battery management strategy in a lead-acid and lithium-ion hybrid battery energy storage system for conventional transport vehicles. Energies. 2022; 15 (7): 2577.
19. Garche J, Moseley PT, Karden E. Lead-acid batteries for hybrid electric vehicles and battery electric vehicles. In: Scrosati B, Garche J, Tillmetz W, editors. Advances in Battery Technologies for Electric Vehicles. Sawston, UK: Woodhead Publishing; 2015. pp, 75–101
20. McKinney BL, Wierschem GL, Mrotek EN. Thermal management of lead-acid batteries for electric vehicles. SAE Trans. 1983: 839–845.
21. Liu W, Placke T, Chau KT. Overview of batteries and battery management for electric vehicles. Energy Rep. 2022; (8): 4058–4084.
22. Cooper A, Moseley P. Progress in the development of lead-acid batteries for hybrid electric vehicles. In: 2006 IEEE Vehicle Power and Propulsion Conference, Windsor, UK, September 6–8, 2006. pp. 1–6.

23. Conte FVo. Battery and battery management for hybrid electric vehicles: a review. E & I Elektrotechnik und Informationstechnik. 2006; 23 (10): 424–431.
24. Juang LW, Kollmeyer PJ, Jahns TM, Lorenz RD. System identification-based lead-acid battery online monitoring system for electric vehicles. In: 2010 IEEE Energy Conversion Congress and Exposition, Atlanta, GA, USA, September 12–16, 2010. pp. 3903–3910.
25. Oman H. On-board energy and power management on electric vehicles: effect of battery type. In: 17th DASC. AIAA/IEEE/SAE. Digital Avionics Systems Conference. Proceedings (Cat. No. 98CH36267), Bellevue, WA, USA, October 31–November 7, 1998. pp. 143/1–143/6.
26. Bullock KR, Brilmyer GH, Wierschem GL. Performance of improved lead acid batteries for electric vehicles. In: Bullock KR, Pavlov D, editors. Proceedings of the Symposium on Advances in Lead-Acid Batteries. Vol. 84. No. 14. Pennington, NJ, USA: Electrochemical Society; 1984.
27. Liu Y-C. Battery management systems for improving battery efficiency in electric vehicles." World Electric Vehicle J. 2010; 4 (2): 351–357.
28. Kasprzyk L. Modelling and analysis of dynamic states of the lead-acid batteries in electric vehicles. Eksploatacja i Niezawodność. 2017; 19 (2): 229–236.
29. Singh A, Karandikar PB, Kulkarni NR. Mitigation of sulfation in lead acid battery towards life time extension using ultra capacitor in hybrid electric vehicle. J Energy Storage. 2021; 34: 102219.
30. Vasebi A, Bathaee SMT, Partovibakhsh M. Predicting state of charge of lead-acid batteries for hybrid electric vehicles by extended Kalman filter. Energy Convers Manage 2008; 49 (1): 75–82.

